Fermi gas energetics in low-dimensional metals of special geometry

Avto Tavkhelidze,[a] Vasiko Svanidze, and Irakli Noselidze
Tbilisi State University, Chavchavadze Avenue 13, 0179 Tbilisi, Georgia

(Received 2 January 2007; accepted 6 June 2007; published 6 July 2007)

Changes in the metal properties caused by periodic indents in the metal surface were studied within the limit of quantum theory of free electrons. The authors show that due to destructive interference of de Broglie waves, some quantum states inside the low-dimensional metal become quantum mechanically forbidden for free electrons. Wave-vector density in k space is reduced dramatically. At the same time the number of free electrons does not change, as the metal remains electrically neutral. Because of the Pauli exclusion principle, some free electrons must occupy quantum states with higher wave numbers. The Fermi vector and Fermi energy of low-dimensional metal increase, and consequently, the work function decreases. In the experiment, the magnitude of the effect is limited by the roughness of the metal surface. A rough surface causes scattering of the de Broglie waves and compromises their interference. Recent experiments demonstrated a reduction of work function in thin metal films having periodic indents in the surface. Experimental results are in good qualitative agreement with the theory. This effect could exist in any quantum system comprising fermions inside a potential-energy box of special geometry. © *2007 American Vacuum Society.* [DOI: 10.1116/1.2753852]

I. INTRODUCTION

Recent developments of nanoelectronics enable the fabrication of structures with dimensions comparable to the de Broglie wavelength of a free electron inside a solid. This new technical capability makes it possible to fabricate some microelectronic devices such as resonant tunneling diodes and transistors, superlattices, quantum wells, and others[1] based on the wave properties of the electrons. In this article, we discuss what happens when regular indents, which cause interference of de Broglie waves, are fabricated on the surface of a thin metal film. We will study the free electrons inside a rectangular potential-energy box with indented wall and compare the results to the case of electrons in a box with plane walls. We have shown that modifying the wall of a rectangular potential-energy box leads to an increase of the Fermi energy level. Results obtained for the potential-energy box were extrapolated to the case of low-dimensional metals (thin metal films). The experimental possibility of fabricating such indents on the surface of a thin metal film was studied. Practical recommendations regarding dimensions and shape of the indents are given. In addition, the influence of nonregularities of thin metal films, such as the presence of granules inside the film and the roughness of surface of the film, was studied.

II. ELECTRONS IN A POTENTIAL-ENERGY BOX WITH AN INDENTED WALL

We begin with the general case of electrons inside a potential-energy box. Assume a rectangular potential-energy box with one of the walls modified as shown in Fig. 1. Let the potential energy of the electron inside the box volume be equal to zero, and that outside the box volume be equal to infinity. The indents on the wall have the shape of strips having depth a and width w. Let us name the box shown on Fig. 1 as indented potential-energy box (IPEB) to distinguish it from the ordinary potential-energy box (PEB) having plane walls.

The time independent Schrödinger equation for electron wave function inside the PEB has the form

$$\nabla^2\Psi + (2m/\hbar^2)E\Psi = 0. \tag{1}$$

Here, Ψ is the wave function of the electron, m is the mass of the electron, and E is the energy of the electron. Let us rewrite Eq. (1) in the form of the Helmholtz equation,

$$(\nabla^2 + k^2)\Psi = 0, \tag{2}$$

where k is wave vector, $k = \sqrt{2mE}/\hbar$.

Once the indent depth a in our particular case is supposed to be much less than the thickness of the metallic film $a \ll L_x$, we can use the volume perturbation method to solve the Helmholtz equation.[2] The idea is as follows: The whole volume is divided in two parts, the main volume (MV) and the additional volume (AV). The MV is supposed to be much larger than the AV, and it defines the form of solutions for the whole composite volume. Next, solutions of the composite volume are searched in the form of solutions of the MV. The method is especially effective in the case where the MV has a simple geometry, for example, a rectangular geometry, allowing separation of the variables. In our case, the whole volume in Fig. 1 can be divided in two, as shown in Fig. 2. We regard the big rectangular box as the MV and the total volume of strips as the AV. The MV has dimensions L_x, L_y, and L_z. The solutions of Eq. (2) for such a volume are well known. Because of the rectangular shape, solutions are found by using the method of separation of variables. The solutions are plane waves having a discrete spectrum,

[a]Electronic mail: avtotav@geo.net.ge

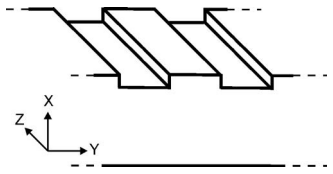

FIG. 1. Three-dimensional view of indented potential-energy box.

$$k_n^{mx} = \pi n/L_x, \quad k_j^{my} = \pi j/L_y, \quad k_i^{mz} = \pi i/L_z. \tag{3}$$

Here, k^{mx}, k^{my}, and k^{mz} are the x, y, and z components of wave vectors of the MV and $n,m,i=1,2,3,\ldots$. In the same manner the spectrum of the single strip of the AV is the following:

$$k_p^{ax} = \pi p/a, \quad k_q^{ay} = \pi q/w, \quad k_i^{az} = \pi i/L_z. \tag{4}$$

Here, k^{ax}, k^{ay}, and k^{az} are components of wave vectors of one strip of AV, $p,q=1,2,3,\ldots$, and a and w are dimensions of the strip, as shown on Fig. 2. Suppose the MV has a length of L_y in the Y direction. Let us assume $L_y=l\cdot 2w$, where l is an integer. Once solutions of the MV are periodic in the Y direction, and AV contain periodic in Y direction strips, we can find solutions of the composite volume by matching a single strip to the MV. Let $\Psi_m(x,y,z)$ be the wave function of electrons in the MV and $\Psi_a(x,y,z)$ be the wave function in the AV. The matching conditions will be $\Psi_m=\Psi_a$ and an equation of partial derivatives from two sides for all points of the connection area. In the MV, $\Psi_m=0$ for all points of the walls. In the AV, $\Psi_a=0$ for all points of the walls. Obviously, $\Psi_m=\Psi_a$, for all points of the connecting area, is satisfied automatically. Equations of partial derivatives $\partial\Psi_m/\partial x=\partial\Psi_a/\partial x$, $\partial\Psi_m/\partial y=\partial\Psi_a/\partial y$, $\partial\Psi_m/\partial z=\partial\Psi_a/\partial z$ lead to equations of wave-vector components in the two volumes, $k^{mx}=k^{ax}$, $k^{my}=k^{ay}$, and $k^{mz}=k^{az}$. The volumes in Fig. 2 have the same spectra along the Z axis [Eqs. (3) and (4)]. Obviously, the matching of two volumes occurs automatically in the Z direction, $k_i^{mz}=k_i^{az}=\pi i/L_z$. Along the X direction, we must match two discrete spectra ($k_n^{mx}=\pi n/L_x$ and $k_p^{ax}=\pi p/a$),

$$k_{np}^{cx} = k_n^{mx} \cap k_p^{ax} = (\pi n/L_x) \cap (\pi p/a). \tag{5}$$

Here, k_{np}^{cx} is the spectrum of the composite volume in the X direction. Equation (5) means that during matching, we have to select wave vectors from the spectrum of the MV, having n such that, when multiplied by a/L_x, it returns a natural number q. The matching condition could be written as $n(a/L_x)\in N$. To obtain an analytical result, let us find the maximum density of solutions for the composite volume in the X direction. According to Eq. (5), the spectrum for the composite volume is the intersection of the spectrum of the MV and the spectrum of the AV. Because $L_x>a$, the spectrum of the MV is more dense than the spectrum of the AV. The intersection of the large solution set (the spectrum of the MV) and the small solution set (the spectrum of the AV) is a maximum when the small set is a subset of the large set. We can write $(\pi q/a)\in(\pi n/L_x)$ and $(L_x/a)q\in n$. The last situation can happen only when $L_x/a=o$, where o is natural number. Once we maximize the number of solutions, we can write

$$k_{np}^{cx} = \pi p/a, \tag{6}$$

and use Eq. (6) for further calculations, keeping in mind that we are calculating the case of the maximum solution set (or spectrum density).

Next we will match solutions of two rectangular volumes along the Y direction in the same way,

$$k_{jq}^{cy} = k_j^{my} \cap k_q^{ay} = (\pi j/L_y) \cap (\pi q/w). \tag{7}$$

Here, k_{jq}^{cy} is the spectrum of the composite volume in Y direction. We maximize solutions just as we did for the X direction and find

$$k_{jq}^{cy} = \pi q/w. \tag{8}$$

Finally, we have the following spectrum for the composite volume:

$$k_{np}^{cx} = \pi p/a, \quad k_{jq}^{cy} = \pi q/w, \quad k_{ii}^{cz} = \pi i/L_z. \tag{9}$$

Let us rewrite the spectra for PEB and IPEB

$$k_n^x = \pi n/L_x, \quad k_j^y = \pi j/L_y, \quad k_i^z = \pi i/L_z, \quad \text{for PEB}, \tag{10a}$$

and

$$k_p^x = \pi p/a, \quad k_q^y = \pi q/w, \quad k_i^z = \pi i/L_z, \quad \text{for IPEB}. \tag{10b}$$

In the last formulae, we skip some working indices used in this section to simplify the presentation.

Formulae (10a) and (10b) are obtained using the volume perturbation method for solving of the Helmholtz equation. This method assumes that the AV is much less than the MV $(a/2L_x)\ll 1$. Special attention should be paid to the limit of very low a and w. Case a, $w\to 0$ has the following physical interpretation. Standing waves in the MV ignore the AV because of wave diffraction on it. If we assume that the wave ignores nonregularities with dimensions less than its wavelength, we must make the following corrections in formulae (10b). It is valid for $k^x>2\pi/a$ and $k^y>2\pi/w$ for $p,q=2,3,4,\ldots$. For the range $0<k^x<2\pi/a$ and $0<k^y<2\pi/w$, Eq. (10a) should be used for IPEB instead of Eq. (10b). In practice, dimensions a and w are such that only the first few k should be added to Eq. (10b).

For the case of large $a/2L_x$, other methods were used. The general solution of Eq. (2) in such a complicated geometry

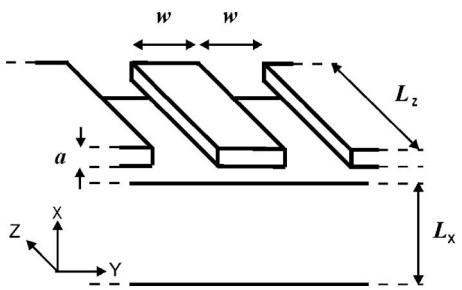

FIG. 2. Potential-energy box with indented wall divided into two volumes. Main volume has dimensions L_x, L_y, and L_z, and one of the strips of the additional volume has dimensions a, w, and L_z.

exhibits several problems. A complicated surface shape does not allow finding an orthogonal coordinate system that will allow separation of variables. Therefore, boundary conditions may be written only in the form of piecewise regular functions. A general solution of Eq. (2) usually contains infinite sums. However, there are methods[2] that allow one to obtain a dispersion equation and to calculate the wave vector. The Helmholtz equation is frequently used for calculating the electromagnetic field in electromagnetic resonator cavities, waveguides, and delay lines. We found the following similarities between the electron wave function inside the IPEB and electromagnetic field inside electromagnetic delay lines. First, our geometry matches the geometry of a corrugated waveguide delay line.[3] Second, the same Eq. (2) is used to describe both cases. Third, the boundary condition for the electromagnetic wave inside the corrugated waveguide $\epsilon=0$ (here, ϵ is the electric component of the electromagnetic wave) for walls of a conductive waveguide exactly matches the boundary condition for electrons, $\Psi=0$ outside the metal. Fourth, any wave can be presented as the sum of plane waves in both cases. We also found that similar analogies are described in the literature.[4] Therefore, for the case of high a, we used the method of solving the Helmholtz equation inside the corrugated waveguides.[2,3] This method is based on solving a transcendental equation. We found numerical solutions for the transcendental equation for high $a/2L_x$ and obtained the same result, namely, the reduction of the spectrum density for IPEB relative to PEB.

For very thin films $L_z \gg L_x$, w, it is expected that our structure will not exhibit quantum features in the Z direction. Therefore, it is reasonable to consider a model of the electron motion in a two-dimensional (2D) region delimited by the line $X=0$ from one side, and a periodic curve on the opposite side. In that case, we can consider the 2D Helmholtz equation and use special methods on solving. Specifically, we used the boundary integral method (BIM), which is especially effective for the low-energetic part of the spectrum and has been widely employed for studying 2D nanosystems.[5]

The BIM method implies consideration of an appropriate integral equation instead of the Helmholtz equation. We have applied the corresponding numerical algorithm[6] to a finite number of periods and calculated the lowest ten energy levels. We note that computation of higher energy levels with reasonable accuracy demands rapidly increasing machine time. The obtained spectrum of transverse wave vectors also shows a reduction in spectral density.

At the end of this section, it is worth noting that the above-discussed effect of the energy-spectrum reduction is closely related to the so-called quantum billiard problem. The 2D system studied represents a modification of the quantum billiard problem. Unlike the circle and rectangular billiards, the corrugated boundary makes the system under consideration nonintegrable. This means that the number of degrees of freedom exceeds the number of constants of motion. Such billiards constitute chaotic systems. The distinction between the spectra of chaotic and nonchaotic (regular) systems is exhibited by an energy level spacing distribution.[6,7] Namely, consecutive energy levels are likely to attract each other in the case of an integrable system, whereas they repel each other in the case of a chaotic system.

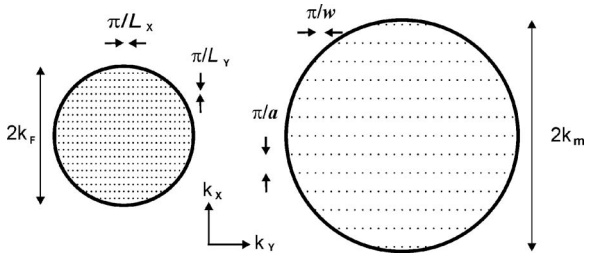

FIG. 3. Section of Fermi sphere is k space for PEB (left) and IPEB (right).

III. FREE ELECTRON IN LOW-DIMENSIONAL METAL WITH MODIFIED WALL

To investigate how periodic indents change quantum states inside the low-dimensional metal, we will use a quantum model of free electrons. Free electrons inside the metal form a Fermi gas. Cyclic boundary conditions of Born-Carman,

$$k_n^x = 2\pi n/L_x, \quad k_j^y = 2\pi j/L_y, \quad k_i^z = 2\pi i/L_z, \tag{11}$$

are used instead of Eq. (3). Here, $n,j,i=0,\pm1,\pm2,\pm3,\ldots$. The result of the theory is a Fermi sphere in k space. All possible quantum states are occupied until k_F at $T=0$. However, for $T>0$, there are two types of free electrons inside the Fermi gas. Electrons with $k \approx k_F$ interact with their environment and define the transport properties of metals such as charge and heat transport. Electrons with $k \ll k_F$ do not interact with the environment because all quantum states nearby are already occupied by other electrons (it becomes forbidden to exchange small amounts of energy with the environment). Such electrons are ballistic and have formally infinite mean free path. This feature allows us to regard them as planar waves, traveling between the walls of the metal (if the distance between walls is not too great). Further, we will concentrate on such ballistic electrons. Once we work with electrons with infinite (or very long) mean free paths, we can regard the low-dimensional metal as a potential-energy box and extrapolate calculations of the previous section to it.

We start by comparing the volume of an elementary cell in k space for thin metal films with and without periodic indents. From Eqs. (10a), (10b), and (11), we have

$$dV_k = 8\pi^3/(L_x L_y L_z) \quad \text{and} \quad dV_{k\ \mathrm{in}} = 8\pi^3/(awL_z). \tag{12}$$

Here, dV_k is the volume of an elementary cell in k space for a plain film, and $dV_{k\ \mathrm{in}}$ is the volume of an elementary cell in k space for an indented film. For the ratio of volumes, we get $(dV_k/dV_{k\ \mathrm{in}})=(aw)/(L_x L_y)$. Because each electron occupies more volume of the k space in the case of indented metal, some electrons must occupy quantum states with $k>k_F$. Consequently, the Fermi wave vector and the corresponding Fermi energy level of an indented metal film will increase as in Fig. 3.

Next, we calculate the maximum wave vector k_m at $T=0$ for an indented metal film. Assume that the metal lattice is cubic, the metal is single valence and the distance between atoms is d. The volume of the metal box shown in Fig. 1 is

$$V = L_y L_z (L_x + a/2). \tag{13}$$

The number of atoms inside the metal of that volume is $s = V/d^3$. The number of free electrons is equal to s and we have

$$s = L_y L_z (L_x + a/2)/d^3 \tag{14}$$

for the number of free electrons. The total volume occupied by all electrons in k space will be

$$V_m = (s/2) dV_{k\ \mathrm{in}} = (4/3)\pi k_m^3. \tag{15}$$

Here, k_m is the maximum possible k in the case of the indented metal film, and V_m is the volume of the modified Fermi sphere in k space. Each k contains two quantum states occupied by two electrons with spins of $1/2$ and $-1/2$. That is why coefficient 2 appeared in Eq. (15). From Eqs. (12)–(15), we calculate the radius of modified Fermi sphere as

$$k_m = (1/d)[3\pi^2 (L_y (L_x + a/2)/(aw)\ ]^{1/3}. \tag{16}$$

The radius of a Fermi sphere k_F for an ordinary metal film does not depend on its dimensions and equals $k_F = (1/d)(3\pi^2)^{1/3}$. Comparing the last equation with Eq. (16), we have

$$k_m = k_F [L_y (L_x + a/2)/(aw)]^{1/3}. \tag{17}$$

Equation (17) shows the increase of the radius of the Fermi sphere in the case of a low-dimensional, indented metal film in comparison with the same metal film with a plane surface (Fig. 3). According to $E \sim k^2$, the Fermi energy in the low-dimensional metal film with the indented surface will relate to the Fermi energy in the same metal film with the plane surface as follows:

$$E_m = E_F [L_y (L_x + a/2)/(aw)]^{2/3}. \tag{18}$$

If we assume $a \ll L_x$, Eq. (18) can be rewritten in the following simple form:

$$E_m = E_F (L_x L_y/aw)^{2/3}. \tag{19}$$

As mentioned above, the case of a, $w \to 0$ has a different physical interpretation (wave diffraction on small volume) and should not be regarded as a singularity in Eq. (19). The next question is what value of L_y should be used in Eq. (19) in the case of infinite length of the structure in the Y direction (Fig. 1). We remember here that wave properties of electrons in solids are limited by the mean free path σ. Consequently the maximum value of L_y is $L_{y\ \max} = \sigma$. Therefore, for the thin film (structure, infinite in the Y direction) we can write

$$E_m = E_F [(L_x/a)(\sigma/w)]^{2/3}. \tag{20}$$

We remember here that the above calculations were made for the case if Eqs. (6) and (8) are valid, or for the case of maximized possible quantum states.

An obvious question emerges: assume we make the ratio $L_x L_y/aw$ high enough for E_m to exceed the vacuum level, what will happen? If we assume that one electron has energy greater than the vacuum level, it will leave the metal. The metal, as a result, will charge positively, and the bottom of the potential-energy box will go down on the energy scale, because the metal is now charged. Once the energy level at the bottom of the potential-energy box decreases, a vacant place for the electron will appear at the top region of the potential-energy box. The electron that left the metal will return because of the electrostatic force and occupy the recently released energy level. Accordingly, E_m will not exceed the vacuum level. Instead, the energy level at the bottom of the potential-energy box will go down exactly to such a distance to allow the potential-energy box to carry all the electrons needed for electrical neutrality of the metal.

In thin metal films, the surface is never ideally plane. The roughness of the surface strongly limits the increase of the Fermi level. These limits will be discussed in more detail in the next section.

The dimensional quantum effects in ultrathin metal films, using a rectangular potential-box model and quantum model of free electrons, were studied in Ref. 8.

IV. PROBLEMS OF PRACTICAL REALIZATION AND POSSIBLE SOLUTIONS

The type of structure discussed could be obtained by depositing a thin metal film on an insulator substrate, and then etching the indents inside the metal film. What are the limitations? The de Broglie wave diffraction will take place on the indents. Diffraction on the indents will lead to the wave "ignoring" the indent, which changes all the calculations above. Consequently, the results obtained are valid only when the diffraction of the wave on the indent is negligible, or $\lambda \ll w$. Here, $\lambda = 2\pi/k_1$ is the de Broglie wavelength of the electron with wave vector k_1. In the case when the indent width is $w > \sigma$, wave properties of the electron will not propagate on many indents along the Y axis. In that case, wave interference will have only local character and the effect will not depend on w and L_y. Values describing the Y dimension will not be included in Eq. (20). This one-dimensional case was analyzed in Refs. 9 and 10.

There are some requirements to the homogeneity of the thin metal film. First, the film structure should be as close to single crystal as possible. This requirement arise, because the free-electron wave function should be continuous through the whole thickness of film $L_x + a$, which means that the metallic film cannot be granular. If the thin metallic film is granular, the wave function will have an interruption on the border of grains, and the indented wall's influence will be compromised. Note that lattice impurities do not influence free electrons with energies $E \ll E_F$. In order to interact with an impurity inside the lattice, an electron should exchange energy (a small amount of energy) with the impurity. That

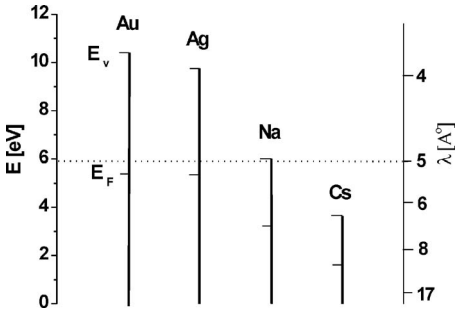

FIG. 4. Energy diagrams of some single-valence metals on the scale of de Broglie wavelength.

type of energy exchange is forbidden because all possible quantum states nearby are already occupied. Because of this, the mean free path of an electron, having energy $E \ll E_F$, is very long. Consequently, the material of the film can have impurities, but the film should not be granular.

Surface roughness should be minimized, because it leads to the scattering of de Broglie waves. Scattering is considerable for the de Broglie wavelengths less than the roughness of the surface. Substrates with a roughness of 5 Å are commercially available. Metal film deposited on such a substrate can also have a surface with the same roughness. The de Broglie wavelength of a free electron at the Fermi level is 5–10 Å in metals. Scattering of the de Broglie waves of electrons having energies $E \approx E_F$ will be considerable. Corresponding energy levels will be smoothed. Smoothing of energy levels decreases the lifetime and leads to continuous energy spectrum, instead of a discrete one. Figure 4 shows Fermi and vacuum levels of some single-valence metals on the energy scale (left Y axis) and simultaneously on the scale of de Broglie wavelength (right Y axis) of the electron calculated from $\lambda = 2\pi\hbar/\sqrt{2mE}$. Figure 4 demonstrates that 5 Å roughness of the surface is enough to eliminate the energy barrier for metals such as Cs and Na. The same 5 Å roughness creates a gap from zero to about the Fermi level in the energy spectrum of metals such as Au and Ag. As a result, it is possible to reduce the work function of Cs and Na to zero, in the case of 5 Å surface roughness; but the same 5 Å roughness on the surface of Au or Ag allows a reduction of the work function of only 0.5–1 eV.

The depth of the indent should be much more than the surface roughness. Consequently, the minimum possible a is 30–50 Å. According to Eq. (20), the minimum possible w will be 300–500 Å. The primary experimental limitation in the case of the structure shown in Fig. 4 is that the ratio $(L_x/a) > 5$, to achieve a maximum work-function reduction. Consequently, the thickness of the metal film should be more than 300 Å. Films of such thickness usually still repeat the substrate surface shape, and film surface roughness will not exceed the roughness of the base substrate. However, the same is not true for metal films with a thickness of 1000 Å and more, because a thick film surface does not follow the surface of the substrate. That puts another limit, 15 $\geqslant (L_x/a) \geqslant 5$, on the dimensions of the film. Other possible structures, such as single crystal, will not be limited by the same requirements.

It should be noted that the spectrum density will change if there is a shift in periodicity of the indents in the Y direction. In experiments, it is difficult to keep exact periodicity, especially in the case of low width of the indent. In such case, neighboring indents will have a different spectrum $k_q^{ay} = \pi q/w$, depending on their individual width w. Then one more spectrum should be included in Eq. (8), and we will have an intersection of three sets instead of two. It will decrease the spectrum density.

And finally there are some limits on the selection of materials that could be used for a thin film. Most metals oxidize under the influence of the atmosphere. Even when placed in a vacuum, metals oxidize with time, because of the influence of residual gases. Typical metal oxides have a depth of 50–100 Å which is considerable on the depth scale discussed. Because of those limitations, gold is the best material that can be used in experiments.

An effect was observed in thin Au and Nb films. Thin films with indented surfaces were fabricated and their work-function reduction was observed.[11] Experimental results are in qualitative agreement with the theory. Particularly, experiments show that work-function reduction strongly depends on the structure of the indented film. Amorphous films show much more reduction in work function than polycrystalline films made from the same material. Work-function reduction in samples depends on the depth of the indents, as predicted by theory. Experiments did not show quantitative agreement with the theory. One of the reasons could be that the effect strongly depends on the structure of the film. In particular, the effect depends dramatically on the value of the mean free path of electrons below the Fermi level. In the theory, we assume that the mean free path of such electrons is much more than film thickness. Most probably we have not realized such a condition in our recent measurements made at $T = 300$ K. The finite roughness of the surface of Au films causes de Broglie wave scattering and reduces the effect. Roughness of the surface is not included in calculations, and it is probably one more reason why we do not have quantitative agreement between experiment and theory.

V. CONCLUSIONS

To investigate a new quantum interference effect in low-dimensional metals, we studied the behavior of free electrons in the potential-energy box of special geometry. It was shown that when periodic indents are introduced in the plain wall of a rectangular potential-energy box, the spectrum density of possible solutions of the Schrödinger equation is reduced dramatically. Once the number of possible quantum states decreases, electrons must occupy higher energy levels because of the Pauli exclusion principle. Results obtained for electrons in the modified potential-energy box were extrapolated to the case of the free ballistic electrons inside the low-dimensional metal film. The electron distribution function of low-dimensional metal changes. Fermi energy in-

creases, and consequently, work function decreases. Limiting factors of the effect are metal surface roughness and the finite mean free path of ballistic electrons. Because surface roughness is a limiting factor, the magnitude of the effect will be higher for materials having a low value of Fermi energy and low value of work function. Because electron mean free path is also a limiting factor, the effect will be higher in the case of a single crystal or amorphous structure of the film. Recent experiments demonstrate good quantitative agreement with theory. Increase in the Fermi level and the corresponding decrease of the work function of the thin films will have practical use for devices working on the basis of electron emission and electron tunneling. In addition, such layers will be useful in the semiconductor industry, particularly for the structures in which contact potential difference between two layers plays an important role.

ACKNOWLEDGMENTS

The authors thanks Stuart Harbron for useful discussions. Work is financed and supported by Borealis Technical Limited, assignee of corresponding U.S. patents (7,166,786; 7,074,498; 6,281,514; 6,495,843; 6,680,214; 6,531,703; and 6,117,344).

[1] *Physics and Applications of Semiconductor Quantum Structures*, edited by Yao J.-C. Woo (IOP, Bristol, 2001).
[2] V. M. Sedykh, *Waveguides With Cross Section of Complicated Shape* (Kharkhov University Press, Kharkov, 1979), p. 16; William S. C. Chang, *Principles of Lasers and Optics* (University of California, San Diego, 2005).
[3] R. S. Elliott, IRE Trans. Antennas Propag. **2**, 71 (1954).
[4] R. A. Silin and B. P. Sazonov, *Delaying Systems* (Soviet Radio, 1966), p. 395.
[5] G. Chen and J. Zhou, *Boundary Element Methods* (Academic, San Diego, 1992).
[6] I. Kosztin and K. Schulten, Int. J. Mod. Phys. C **8**, 293 (1997).
[7] F. Haake, *Quantum Signatures of Chaos* (Springer, Berlin, 1991).
[8] V. V. Pogosov, V. P. Kurbatsky, and E. V. Vasyutin, Phys. Rev. B **71**, 195410 (2005); V. P. Kurbatsky and V. V. Pogosov, Vacuum **74**, 185 (2004).
[9] A. Tavkhelidze, Proceedings the Sixth International Workshop "From Andreev Reflection to the International Space Station," Björkliden, Kiruna, Sweden, 4–11 April 2002 (unpublished); http://fy.chalmers.se/%7Ef4agro/6WARISS/DOC/Tavkhelidze.htm
[10] A. Tavkhelidze and S. Harbron, U.S. Patent No. 7,074,498 (11 July 2006).
[11] A. Tavkhelidze *et al.*, J. Vac. Sci. Technol. B **24**, 1413 (2006).